Proceedings of the 28th IEEE
EMBS Annual International Conference
New York City, USA, Aug 30-Sept 3, 2006

Comparison of brain white matter fiber orientation measurements based on diffusion tensor imaging and light microscopy

Adam W. Anderson, Ann S. Choe, Iwona Stepniewska, and Daniel C. Colvin

***Abstract*—Diffusion tensor magnetic resonance imaging (MRI) was used to estimate white matter fiber orientations in fixed brain specimens. The specimens were subsequently sectioned, stained for myelinated fibers, and imaged with light microscopy. The MRI data were registered with the micrographs, allowing direct comparison of fiber orientation estimates between the two methods. Fiber orientation was measured in regions of interest in the frontal lateral corpus callosum. The results of diffusion MRI and light microscopy agreed within 2 degrees—the difference was not statistically significant.**

I. Introduction

Measurements of anisotropic water diffusion in brain tissue provide the basis for estimates of the orientation and integrity of white matter fiber bundles [1]. These have been used to reconstruct fiber pathways in the brain and characterize white matter injury in a wide range of diseases [2]. Although several important theoretical limitations to diffusion tensor imaging (DTI) have been identified (those due to image noise and partial volume averaging, for example), little is known about how well DTI represents fiber microstructure in the brain. The aim of this work was to make direct comparisons of axon fiber structure measured with DTI and light microscopy in the brain of a non-human primate, the owl monkey, *ex vivo*.

II. Methods

A. Diffusion MRI

Fixed, intact brain specimens (obtained from a separate project, approved by the Vanderbilt University Animal Use Committee) were scanned in a 9.4 Tesla, 21 cm bore magnet controlled with a console from Varian Instruments (Walnut Creek, CA). A multi-slice pulsed gradient, spin echo pulse sequence (TE = 31ms, TR = 17.1s, b = 0 and 1300s/mm^2 in each of 21 diffusion gradient directions, 132 slices) was used to acquire diffusion weighted images at 300 micrometer isotropic resolution. The images were filtered using a nonlinear anisotropic smoothing algorithm that preserves contrast boundaries [3]. The diffusion tensor was calculated in each image voxel using weighted linear least squares estimation.

B. Light microscopy

Brain specimens (which had been perfused with saline followed by 4% paraformaldehyde in phosphate buffer) were soaked in 30% sucrose for 24 hours, frozen, and cut into 50 micrometer coronal sections using a microtome. A digital camera mounted above the microtome was used to photograph the frozen tissue block prior to cutting every third section (i.e., the through-plane resolution of the photographic data was 150 micrometers). Alternating sections were stained for myelinated fibers [4] and mounted for light microscopic analysis. Images of the stained sections were acquired at 0.5x, 1x, 2x, 4x, 10x, and 20x magnification using a Nikon DXM1200F digital camera mounted on a Nikon E-800 microscope.

C. Registration of image data

Diffusion tensor data were registered to the high resolution light microscopy images using a multi-step procedure. First, the (non-diffusion weighted) MR images were assembled into a 3D image volume. The photographic images of the frozen block were similarly combined in a 3D volume (after removing the image background). The MR data were registered to the tissue block data using both rigid and non-rigid transformations calculated by the Adaptive Bases Algorithm, ABA [5]. Tissue block images were registered to low magnification (0.5x) images of the corresponding section using 2D rigid and non-rigid transformations also calculated with ABA. The transformations were combined to establish corresponding points in the light microscopy image and MR image space. Tensors were copied to the appropriate points in the light microscopy image space then rotated according to the 'preservation of principal directions' scheme [6].

Finally, high resolution light microscopic images were registered with lower resolution images of the same section. This was accomplished by minimizing the normalized mutual information as a function of in-plane translations of the higher resolution image in the space of the lower

This work was supported in part by grants from the National Institutes of Health (1RO1 EB002777 and 1S10 RR17799).

A. W. Anderson is with the Biomedical Engineering Department and Institute of Imaging Science, Vanderbilt University, Nashville, TN 37232 USA (phone: 615-322-8353, fax: 615-322-0734; email: adam.anderson@vanderbile.edu).

A. S. Choe is also with the Biomedical Engineering Department and Institute of Imaging Science, Vanderbilt University, Nashville, TN 37232 USA (email: ann.s.choe@vanderbilt.edu).

I. Stepniewska is with the Psychology Department, Vanderbilt University, Nashville, TN 37232 (email: iwona.stepniewska@vanderbilt.edu).

D. C. Colvin is with the Physics Department and Institute of Imaging Science, Vanderbilt University, Nashville, TN 37232 (email: daniel.c.colvin@vanderbilt.edu).

resolution image. High resolution (and hence small field of view) microscope images, e.g., 20x, were registered with 10x, 4x, 2x, 1x, and 0.5x images in succession. The relative scaling of images at different magnifications was determined in a separate experiment by imaging a scale bar. Tensors were then rendered in the high magnification microscope image space using the derived low-to-high magnification image space coordinate translations.

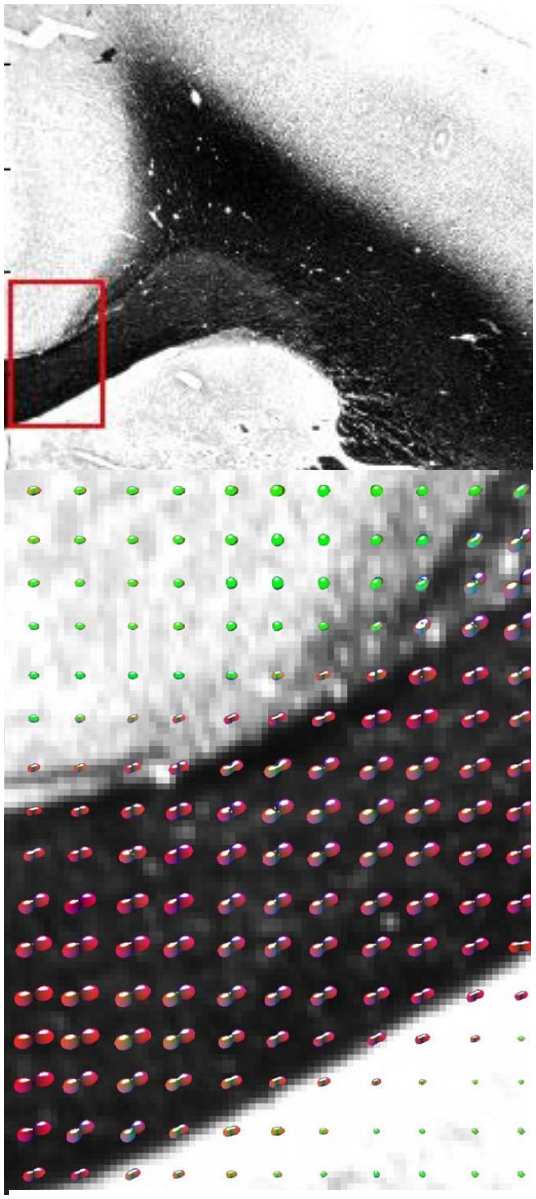

Fig. 1. Low resolution micrograph of a myelin stained section from the owl monkey brain (*top*). The region outlined in red is shown with the corresponding diffusion surfaces (*bottom*).

D. Comparison of fiber orientation data

The transformed tensors were diagonalized in-plane and the principal eigenvector was determined at each sampled point in the high resolution image space. The dominant direction of myelinated fibers was determined using the Radon transform of the micrographs [7]. These independent measures of fiber orientation were then compared. Note that the diffusion MRI data do not influence the estimated coordinate transformation, but are registered according to other image data. For visualization, the tensor data are interpolated to a spatial resolution of 120 micrometers.

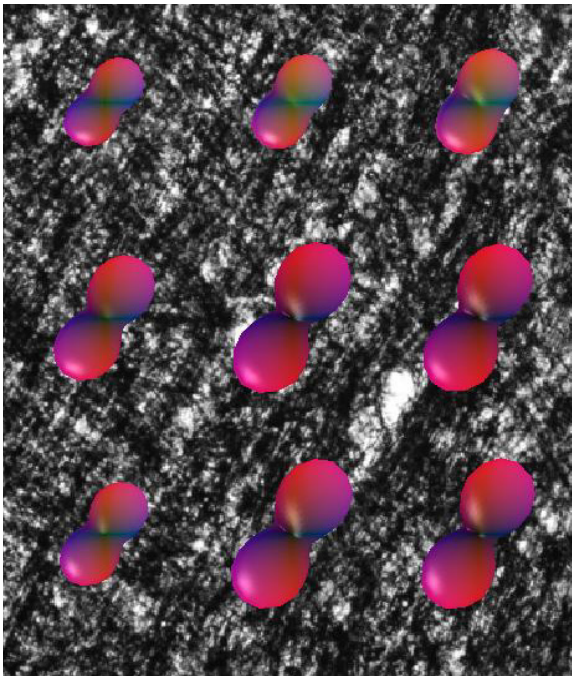

Fig. 2. High resolution image of myelin stained fibers with registered diffusion profiles. The field of view of the image is approximately 370 micrometers.

III. Results

An example of diffusion tensors registered with a light micrograph of a myelin stained section is shown in Fig. 1. The diffusion tensor is rendered as a diffusion surface (i.e., the distance from the origin to the surface in a given direction is proportional to the diffusivity of water in that direction). The long axis of the diffusion surface should lie parallel to the underlying axon bundles. The surfaces are color-coded to show the anatomical direction of fastest diffusion (red => fast diffusion in the right/left direction, green => anterior/posterior, blue => superior/inferior). Figure 1 shows a segment of the corpus callosum (red, or predominantly right/left fibers) passing under the cingulum bundle (green, or anterior/posterior fibers).

Myelinated fibers and diffusion surfaces (at a more lateral location along the corpus callosum) are shown at higher spatial resolution in Fig. 2. The dominant fiber orientation (measured counterclockwise from the horizontal axis in this image) based on the analysis of the myelin stained image is 59 +/- 8 degrees. The principal eigenvector of the in-plane

diffusion tensor is at 61 +/- 5 degrees. The difference between the measurements is not significant ($p = 0.7$).

IV. Discussion and conclusions

These measurements show excellent agreement between fiber orientation estimates by diffusion MRI and light microscopy. To the best of our knowledge, this is the first demonstration of the accuracy of DTI estimates of microscopic fiber orientation in the central nervous system. Whereas the agreement presented here is encouraging, it is likely to be less satisfactory in regions of more complex fiber geometry (e.g., fiber crossing, bending, or splaying). Similar experiments using high angular resolution diffusion imaging (HARDI) should provide tests of the ability of these more general models of diffusion to represent complex fiber architecture in the brain.

Acknowledgment

The authors would like to thank B Dawant and Y Li for assistance with data registration, and Z Ding for his help in anisotropic smoothing of the MRI data.

References

[1] Mori, S. and P.C. van Zijl, "Fiber tracking: principles and strategies - a technical review," NMR Biomed **15**(7-8): pp. 468-80, 2002.

[2] Horsfield, M.A. and D.K. Jones, "Applications of diffusion-weighted and diffusion tensor MRI to white matter diseases - a review," NMR Biomed **15**(7-8): pp. 570-7, 2002.

[3] Ding, Z., J.C. Gore, and A.W. Anderson, "Reduction of noise in diffusion tensor images using anisotropic smoothing," Magn Reson Med **53**(2): pp. 485-90, 2005.

[4] Gallyas, F., "Silver staining of myelin by means of physical development," Neurol Res **1**(2): pp. 203-9, 1979.

[5] Rohde, G.K., A. Aldroubi, and B.M. Dawant, "The adaptive bases algorithm for intensity-based nonrigid image registration," IEEE Trans Med Imaging **22**(11): pp. 1470-9, 2003.

[6] Alexander, D.C., Pierpaoli, C., Basser, P.J., Gee, J.C., "Spatial transformations of diffusion tensor magnetic resonance images," IEEE Trans Med Imaging, **20**(11): pp. 1131-9, 2001.

[7] Bracewell, R.N., *Two-dimensional imaging*. Englewood Cliffs, New Jersey: Prentice-Hall, 1995.